COMPUTER SIMULATIONS OF LIQUID SILICA: WATER-LIKE THERMODYNAMIC AND DYNAMIC ANOMALIES, AND THE EVIDENCE FOR POLYAMORPHISM

IVAN SAIKA-VOIVOD[1] and PETER H. POOLE[2]

[1]*Department of Physics and Physical Oceanography, Memorial University of Newfoundland, St. John's, NL, A1B 3X7, Canada*
[2]*Department of Physics, St. Francis Xavier University, Antigonish, NS, B2G 2W5, Canada*

CONTENTS

I. INTRODUCTION

The qualitative similarities between water and silica have long been appreciated [1,2]. The molecular structure of both substances is dominated by tetrahedral bonding arrangements under ambient pressure, in both the liquid and the solid states. As a consequence, several of the low-pressure ice phases have isomorphic analogs among the crystalline phases of silica (e.g., ice I_h and tridymite).

The similarities between water and silica also extend to the properties of the liquid and amorphous solid forms. Water and silica are both members of a small set of substances that exhibit a density maximum in the liquid phase [1,2].

In addition, for both substances, when the amorphous solid formed at ambient pressure is compressed, the material collapses to a higher density amorphous solid over a relatively narrow range of pressure [3–5]. Such "polyamorphic" behavior of the amorphous solid has been interpreted, in the case of water, as a subglass transition manifestation of an underlying thermodynamic instability in the supercooled liquid, specifically, a liquid–liquid phase transition (LLPT) occurring without a change in the chemical composition [6–8].

As a consequence of these similarities, silica was one of the first substances to be examined for an LLPT after the initial proposal that such a phenomenon occurs in supercooled water [9]. Because of the considerable challenges associated with the determination of the equation of state of real molten silica over the required range of pressure P and temperature T, computer simulations of silica-like models have played a central role in addressing the question of whether an LLPT might occur in this system.

Here, we review the findings of simulation studies of silica related to the phenomena of polyamorphism and LLPTs. As we discuss below, these simulation studies provide ample evidence that the thermodynamic and dynamical behavior of liquid silica follow the pattern of anomalies that are well known in the case of water. However, simulations have yet to provide unequivocal evidence for an LLPT in silica. Hence, there remains important work to be carried out on this system.

II. SIMULATIONS: RIGID-ION MODELS OF SILICA

A large number of interaction potentials have been formulated for modeling silica interactions in computer simulations. In this review, we will focus primarily on results obtained using so-called 'rigid-ion' models, in which silicon and oxygen atoms are modeled essentially as charged soft spheres. These interaction potentials consist of a sum of Coulombic interactions and repulsive interactions of the Born–Mayer–Huggins form [10]. The long-range nature of the Coulombic interactions are typically treated using Ewald summation. The specific parametrizations of the rigid-ion approach that we will discuss below are that of Wookcock, Angell, and Cheeseman (WAC) [11] and van Beest, Kramer, and van Santen (BKS) [12].

The WAC and BKS potentials ignore the polarizability of the O and Si atoms. These potentials also ignore the covalent nature of the bonding occurring in silica, and thus lack, for example, any explicit three-body interactions such as bond-angle bending terms. As a consequence, significant quantitative discrepancies occur between the behavior of these models and the real silica. However, the simple form of these potentials has a practical advantage in that they facilitate the long simulations required to model the supercooled liquid state, especially as T decreases and relaxation times increase dramatically. These models also provide a stark contrast to the models most commonly used to simulate water, in which O and H atoms

are connected into rigid molecular units, with a nearly perfect tetrahedral angle built into the shape of the molecule. The WAC and BKS models have no explicit propensity for tetrahedral bonding built into the potential. The ability of these models to form tetrahedral structures arises spontaneously from the combined influences of the relative charge, stoichiometry, and size of the O and Si ions. The fact that rigid molecular models of water and rigid-ion models of silica can both produce a common pattern of thermodynamic and dynamic behavior is a striking demonstration of the robustness of the phenomena common to both systems, and strongly suggests that the common origin of these phenomena is the occurrence of tetrahedral structure, regardless of the details of how this structure arises.

III.   AMORPHOUS SOLID BEHAVIOR

Figure 1 shows the characteristic behavior associated with polyamorphism of a glassy substance. The experimental curve is taken from Ref. [3] and shows the response of the density ρ of silica glass to increasing P at ambient T. In the vicinity of 10 GPa, the density increases relatively quickly over a small range of P, while at both lower and higher P, the compressibility of the material is significantly less. Similar behavior is observed during experimental compression of amorphous ice, and suggests the existence of two distinct forms of the amorphous solid, usually termed simply as the "low-density" and "high-density" amorphous forms [5,13].

Figure 1 also shows the results of simulations of the WAC model of silica, in both the liquid and the amorphous solid forms [9]. When the simulated amorphous solid is compressed isothermally, the characteristic-inflected shape of the P-ρ isotherms
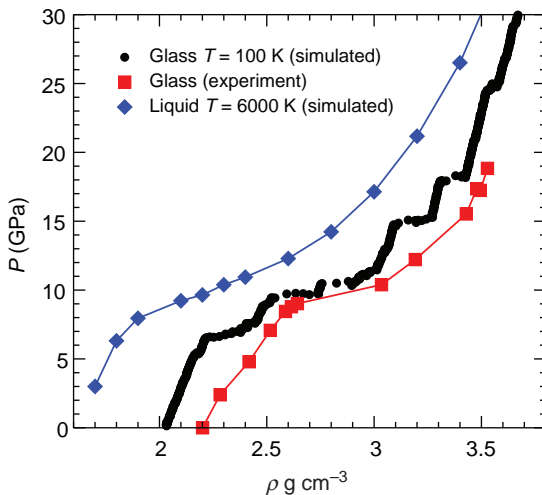
Figure 1. Pressure-volume isotherms for WAC and real silica. Experimental data are from Ref. [3]. The liquid data are shifted upward by 8 GPa to facilitate comparison with the other curves. The protocol for generating the simulated data is described in Ref. [9]

found in experiments on silica glass is qualitatively reproduced, demonstrating the ability of simple rigid-ion models to generate the signature of polyamorphism.

Other simulation studies have aimed at uncovering the structural processes that accompany the compression of silica glass. Experimentally, densification is reversible for a maximum compression of up to 9 GPa. For compressions beyond 12 GPa, decompression back to ambient P results in glass roughly 20% denser than the original. The experiments of Grimsditch showed that the resulting high-density glass is not only denser but also has a different structure from the low-density form [4]. Using another rigid-ion model [14], Lacks suggested that a kinetically hindered first-order amorphous–amorphous transition is responsible for the experimental observations, and that the experiments at higher T may allow direct observation of the first-order transition [15]. Huang and Kieffer, in their detailed structural analysis of a potential incorporating three-body terms and charge transfer [16], found that reversible densification is accomplished by the twisting of Si–O rings, similar to changes accompanying the α–β transition in cristobalite [17]. On the other hand, they found that irreversible densification requires bond rearrangements and is aided by compression at higher T; the P required for the irreversible change is lower for higher T [18].

IV. WATER-LIKE THERMODYNAMIC AND DYNAMIC ANOMALIES

Figure 1 also shows a P-ρ isotherm for the liquid phase of WAC silica. Notably, this isotherm also exhibits an inflection, indicating the presence of a compressibility maximum in the liquid state [19]. In simulations of supercooled liquid water, the same thermodynamic feature occurs, and as T decreases, the compressibility maximum in simulated water grows into a divergence at a critical point [20]. Below the temperature of this critical point, two thermodynamically distinct liquid phases of simulated water occur, each with a distinct density, reflecting the occurrence of a first-order LLPT.

The thermodynamic behavior of both WAC and BKS silica have been examined in the region of the compressibility maximum, and in both cases, the pattern of thermodynamic anomalies that occur have been found to be the same, and analogous to those found in simulation studies of water. An example is shown in Figure 2, that compares the equation of state features of ST2 water [7] with WAC silica [9] in the P–T plane. In both cases, a retracing line of density maxima occurs above a monotonic spinodal boundary. The qualitative similarity of these features, despite the widely different T and P scales, is striking, and certainly suggests that a search for an LLPT in these silica models, of the kind found in water simulations, is justified. This is discussed in the next section.

With regard to dynamical properties, the behavior of silica and water models has also been shown to be in correspondence. A useful concept for studying the relationship between thermodynamics and dynamics, and testing the universality
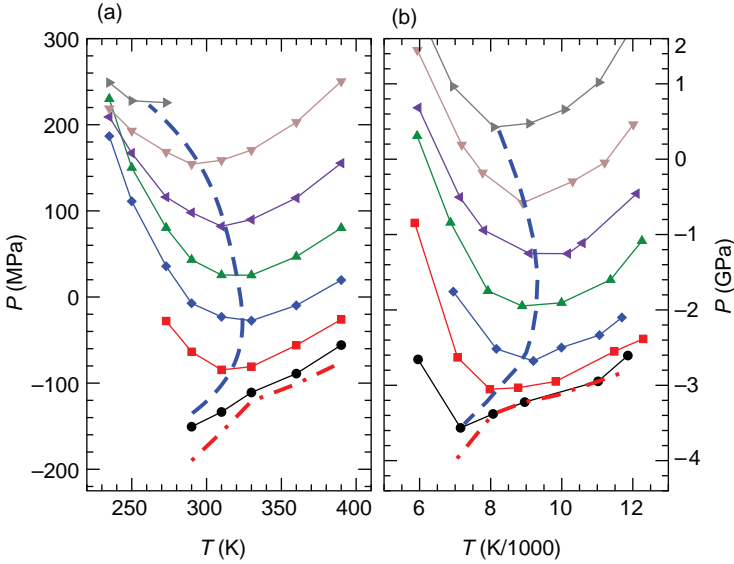
Figure 2. Equation of state features of (**a**) ST2 water and (**b**) WAC silica, projected into the P–T plane. Density maxima (dashed lines) and liquid spinodal boundaries (dot-dashed lines) are shown. Isochores of P as a function of T are shown as symbols joined by thin solid lines. Equally spaced isochores are shown from bottom to top in (a) from $\rho = 0.8$ to 1.1 g/cm^3, and in (b) from $\rho = 1.8$ to 2.4 g/cm^3.

of such relations across liquids, is the potential energy landscape (PEL) formalism [21]. At sufficient supercooling, a liquid system can be thought of as a point hopping between local basins in a $3N$-dimensional potential energy hypersurface. Each basin is associated with a local minimum in potential energy, also termed an inherent structure (IS). In Fig. 3a, the average IS energy e_{IS} is plotted as a function of T for three isochores spanning a wide density range in a slightly modified version of BKS silica [22,23]. The shapes of the curves at the two highest densities are typical of fragile liquids, with $e_{IS} \sim T^{-1}$, behavior that has been shown to result from a Gaussian density of states [24]. A further implication of a Gaussian distribution of IS energies is that the configurational entropy S_c, which is essentially the logarithm of the number of ISs of a given energy, becomes a steeply falling function of T and appears to approach zero at some finite T (Fig. 3b). Through the Adam–Gibbs (AG) relationship [25]

$$\frac{D}{T} = A \exp\left(-\frac{B}{TS_c}\right), \tag{1}$$

a rapidly decreasing S_c accounts for the super-Arrhenius dynamics of fragile liquids, as observed for high-density silica (Fig. 3c and d).
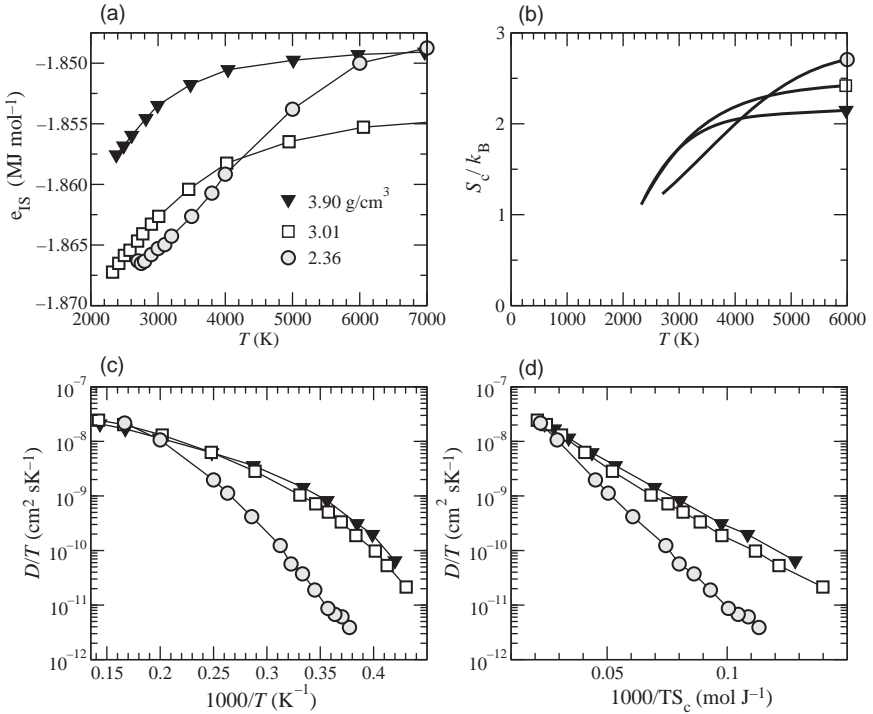
Figure 3. The potential energy landscape and its connection to dynamics. Shown are (**a**) inherent structure energy e_{IS}, (**b**) configurational entropy S_c, and (**c**) diffusivity D as functions of T for three isochores at $\rho = 3.90$ g/cm^3 (5.13 cm^3/mol, triangles), $\rho = 3.01$ g/cm^3 (6.65 cm^3/mol, squares), and $\rho = 2.36$ g/cm^3 (8.50 cm^3/mol, circles). In panel (c), S_c is given per, SiO$_2$ unit. Panel (**d**) shows a test of the Adam–Gibbs relationship. Molar quantities are per mole ions.

For the low-density isochore shown in Fig. 3, e_{IS} exhibits an inflection, arising from a departure from a Gaussian density of states as the liquid approaches a low-energy cutoff [26] associated with a perfect random tetrahedral network. This flattening of the energy produces an inflection in $S_c(T)$, which then presumably approaches a finite value at $T = 0$. This slower variation of S_c with T in turn is responsible for nearly Arrhenius dynamics at low T through Eq. (1). Thus, the inflection in e_{IS}, which is associated with a specific heat peak, is responsible for a crossover in dynamics from super-Arrhenius at high T to Arrhenius at low T. In so far as a locus of specific heat maxima emanates from a possible liquid–liquid critical point located at lower T, it is thus reasonable to expect that the emergent high- and low-density liquid phases associated with this critical point each exhibit distinct dynamics and landscape properties.

While Eq. (1) holds for both water [27] and silica, the density dependence of the diffusivity also tracks that of $S_c(\rho)$ for both liquids [23], though perhaps more strikingly so for water. It would be interesting to compare the dynamics of the two liquids in the tetrahedral regime at low T and low density. For water [28], the dynamics appear to be governed by energy excitations (i.e., bond breaking) above an amorphous ground state, just as in the case of a simpler model network-former, for which the determining nature of bond breaking on dynamics was carefully studied [29,30].

While the above illustrates the similarity in the connections among thermodynamic, structural, and dynamic quantities for silica and water, there are also significant differences, as pointed out by Shell et al. [31]. For example, silica's region in the density–temperature plane of anomalous diffusive behavior (diffusion coefficient increasing with compression) encompasses the structurally anomalous region (translational and tetrahedral order parameters decreasing with compression). The opposite is the case for water. Measures of structural order in silica do not presage the onset of anomalous dynamics as they do for water. The authors of Ref. [31] attribute this difference to the atomic, rather than molecular nature of the potential for silica, and the inherent flexibility in local geometry it confers.

In addition, and despite the similarities in the pattern of thermodynamic and dynamic anomalies displayed by both silica and water models, there remains a significant question relating to the interpretation of the density maximum observed in silica simulations. The density maximum found at ambient P in water simulations is typically within 15% of the experimental value (277 K). However, the temperatures at which a density maximum is observed in silica simulations at ambient P are much higher that the experimental value (1823 K) [1,2]. In the case of BKS silica, the density maximum is approximately 3 times higher in T; in WAC silica it is nearly 5 times higher [19]. Furthermore, the high temperature of the density maximum in simulated silica places it in a regime far above the melting lines for the crystalline phases [32], where the tetrahedral structure of the liquid is highly disrupted, and where the liquid-state dynamics are fragile in character [22,23]. On the other hand, the experimentally observed density maximum in silica occurs in a regime where tetrahedral structure of the liquid is well established, and where the liquid dynamics are decidedly strong.

One explanation of this situation might be that the "water-like" density maximum of silica is not in fact the density maximum that is observed experimentally, but is instead a thermodynamic feature that exists in the high T regime beyond the range of previous experiments. However, such an explanation then implies that the observed density maximum at 1823 K is a distinct feature associated with a well-structured random tetrahedral network. There is precedence for such a possibility, in the fact that a low-temperature density maximum occurs in both ice I_h and LDA ice at approximately 50 K [33]. In addition, if there are two density maxima in liquid silica, they must necessarily be separated by a density minimum. Again, the

analogous behavior may be found in water, where a density minimum has been reported both in simulations [34] and experiment [35]. Clearly, resolution of these questions will require further investigation.

V. EVIDENCE FOR A LIQUID–LIQUID PHASE TRANSITION

While the thermodynamic and dynamical properties of silica and water models are very similar across wide ranges of P and T, the evidence for an LLPT is more highly developed in the case of water models. The evidence for an LLPT is probably most convincing for the case of the ST2 model. The EOS of liquid ST2 water has been extensively studied, and evidence of nonmonotonic isotherms of P versus V, characteristic of behavior in a liquid–liquid coexistence region, have been presented [28]. Most importantly, several evaluations of the free energy surface of ST2 water have confirmed the existence of an LLPT [20,36], although this has recently been challenged [37]. No such direct thermodynamic evidence for a LLPT in silica models has yet been presented, mainly because the temperature range in which a liquid–liquid critical point might be expected is below that which can be reached in straightforward simulations, due to the rapid increase of the relaxation time with decreasing T.

However, several indirect approaches have shown that an LLPT is plausible for silica. For example, Ref. [19] presents an evaluation of the EOS of liquid silica for both the WAC and the BKS models over a wide range of T and P, and then exploits a physically plausible form for extrapolating the isochoric energy to lower T, into the regime in which the liquid cannot be studied in equilibrium by direct simulations. The results provide estimates for the location of the LLPT in WAC and BKS silica that are consistent with the thermodynamic anomalies that occur at higher T and provide a basis for searching for direct evidence of the LLPT in future work.

Another analysis consistent with the occurrence of an LLPT is based on structural properties. Ref. [19] discusses the behavior of $g_5(r)$, defined as the contribution to the usual Si–Si pair distribution function $g(r)$ resulting from Si atoms that are fifth nearest-neighbors (nn) of a given Si atom. In a tetrahedral liquid with an LLPT, the low-density phase is expected to have a local structure in which the fifth nn is excluded from the first coordination shell, while in the high density phase, the fifth nn will be found at distances comparable to the first four nns. An analogous definition for $g_5(r)$ in terms of the fifth nn O atom of a given Si atom should show similar behavior. Plots of $g_5(r)$ evaluated for simulations conducted at constant volume should display a bimodal shape when the system is undergoing phase separation into regions of high- and low-density liquid. Such an analysis is shown for the BKS model in Fig. 4 [38]. This plot shows that $g_5(r)$ does indeed
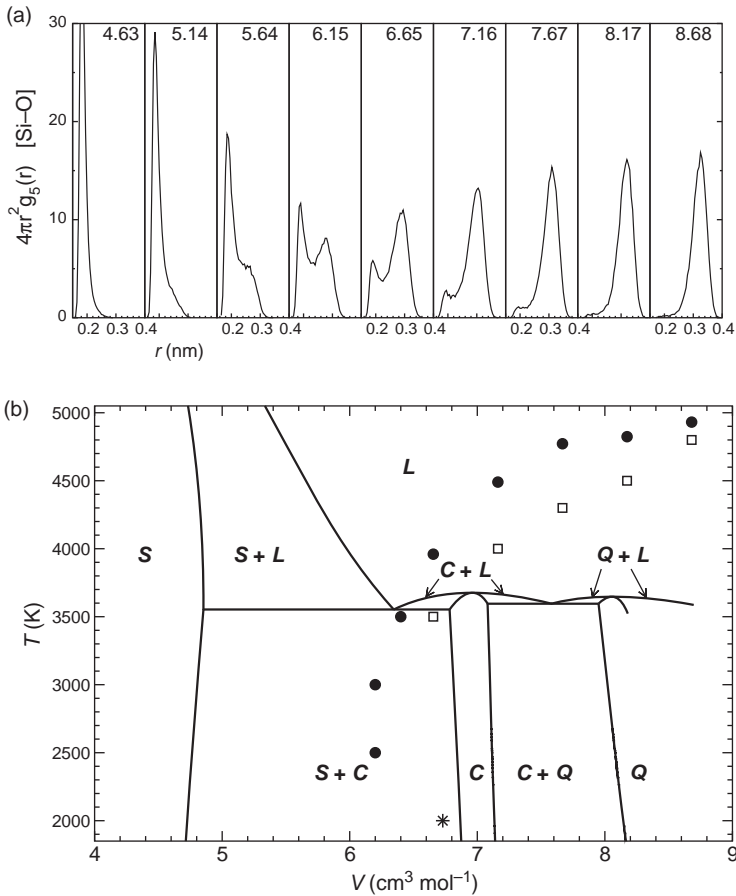
Figure 4. (a) Distributions of distances between a Si atom and its fifth nn O atom at $T = 3000$ K. Subpanels are labelled with molar volumes (cm^3/mol). (b) Projection onto the V–T plane of the coexistence lines for BKS silica separating the liquid (L), quartz (Q), coesite (C), and stishovite (S) phases, obtained as described in Ref. [32]. Density maxima are given by filled circles, and maxima of the isochoric specific heat by open squares. The star locates the position at which evidence for liquid–liquid phase separation was reported in Ref. [19]. (c) A configuration taken from an unequilibrated run at $T = 2000$ K and $V = 6.72$ cm^3/mol [the star in (b)]. Shown are Si atoms, with dark shading indicating a high-density environment where the fifth nn Si atom is within 0.355 nm, the location of the minimum in the Si–Si $g_5(r)$ [19].

become bimodal in the density range that is predicted for the coexistence region of the LLPT.

The above analysis of $g_5(r)$ is not conclusive evidence for an LLPT, because local regions having different structures could form in an isotropic, homogeneous
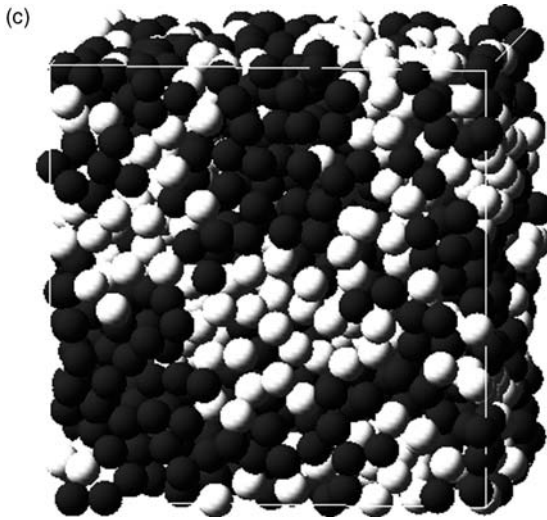
Figure 4.   (*Continued*)

liquid phase without bulk phase separation. Whether or not these local regions phase separate macroscopically depends on the existence of cooperativity in their formation, and how this cooperativity grows as T decreases. A recent study of ST2 water in the vicinity of its LLPT showed that in this case the behavior of $g_5(r)$ is consistent with the location of the LLPT in that model, and provides a practical local order parameter for distinguishing the two liquid phases, and for interpreting the behavior of the liquid above the T of the LLPT in terms of a modified regular solution theory [39]. A similar analysis of the structure of BKS should yield an estimate for the location of the LLPT that could then be searched for in future simulations studies.

VI.   OUTLOOK

As discussed above, the behavior of silica as found in simulations provides a rational basis for anticipating the occurrence of an LLPT in this system, and estimates of the location of the associated critical point have been reported for several silica models. At the same time, the LLPT, if it exists, is located in a challenging regime where the liquid-state relaxation time is large compared to the longest time scales studied in current simulations, and so it may be some time until the question can be addressed definitively. In the meantime, related silica-like systems, such as BeF_2, have significant potential for exploring these phenomena, as has been demonstrated by Angell and coworkers [40] and Chakraborty and coworkers [41]. It also

remains entirely possible that no LLPT occurs in silica (real or simulated) and that this substance exhibits water-like thermodynamic anomalies but without any underlying discontinuities in the thermodynamics of the deeply supercooled liquid. This case would be a realization of the so-called singularity-free scenario [42] for accounting for water-like anomalies. While not as dramatic as an LLPT, confirming singularity-free behavior in silica would do much to deepen our understanding of the range of behavior possible in materials with tetrahedral structure.

REFERENCES

1. C. A. Angell and H. Kanno, *Science* **193**, 1121 (1976)

2. C. A. Angell, P. A. Cheeseman, and S. Tamaddam, *Science* **218**, 885 (1982).

3. H. Sugiura, K.-I. Kondo, and A. Sawaoka, in *High-Pressure Research in Geophysics*, S. Akimoto and M.H. Manghnani eds., Reidel, Dordrecht, 1982, p. 551.

4. M. Grimsditch, *Phys. Rev. Lett.* **52**, 2379 (1984).

5. O. Mishima, L. D. Calvert, and E. Whalley, *Nature* **314**, 76 (1985).

6. P. H. Poole, T. Grande, C. A. Angell, and P. F. McMillan, *Science* **275**, 322 (1997).

7. P. H. Poole, F. Sciortino, U. Essmann, and H. E. Stanley, *Nature (London)* **360**, 324 (1992).

8. O. Mishima and H. E. Stanley, *Nature (London)* **396**, 329 (1998).

9. P. H. Poole, M. Hemmati, and C. A. Angell, *Phys. Rev. Lett.* **79**, 2281 (1997).

10. P. H. Poole, P. F. McMillan, and G. H. Wolf, *Rev. Mineralogy* **32**, 563 (1995).

11. L. V. Woodcock, C. A. Angell, and P. A. Cheeseman, *J. Chem. Phys.* **65**, 1565 (1976).

12. B. van Beest, G. Kramer, and R. van Santen, *Phys. Rev. Lett.* **64**, 1955 (1990).

13. K. Winkel, E. Mayer, and T. Loerting, *J. Phys. Chem. B* **115**, 14141 (2011).

14. S. Tsunekuyi, M. Tsukada, H. Aoki, and Y. Matsui, *Phys. Rev. Lett.* **61**, 869 (1988).

15. D. J. Lacks, *Phys. Rev. Lett.* **84**, 4629 (2000).

16. L. P. Huang and J. Kieffer, *J. Chem. Phys.* **118**, 1487 (2003).

17. L. P. Huang and J. Kieffer, *Phys. Rev. B* **69**, 224203 (2004).

18. L. P. Huang and J. Kieffer, *Phys. Rev. B* **69**, 224204 (2004).

19. I. Saika-Voivod, F. Sciortino, and P. H. Poole, *Phys. Rev. E* **63**, 011202 (2001).

20. F. Sciortino, I. Saika-Voivod, and P.H. Poole, *Phys. Chem. Chem. Phys.* **13**, 19759, 2011.

21. F. Sciortino, *J. Stat. Mech.* **2005**, P05015 (2005).

22. I. Saika-Voivod, P. H. Poole, and F. Sciortino, *Nature (London)* **412**, 514 (2001).

23. I. Saika-Voivod, F. Sciortino, and P. H. Poole, *Phys. Rev. E* **69**, 041503 (2004).

24. S. Sastry, *Nature (London)* **409**, 164 (2001).

25. G. Adam and J. H. Gibbs, *J. Chem. Phys.* **43**, 139 (1965).

26. A. Saksaengwijit, J. Reinisch, and A. Heuer, *Phys. Rev. Lett.* **93**, 235701 (2004).

27. A. Scala, F. Starr, E. La Nave, F. Sciortino, and H. E. Stanley, *Nature (London)* **406**, 166 (2000).

28. P. H. Poole, S. R. Becker, F. Sciortino, and F. W. Starr, *J. Phys. Chem. B* **115**, 14176 (2011).

29. A. J. Moreno, S. V. Buldyrev, E. La Nave, I. Saika-Voivod, F. Sciortino, P. Tartaglia, and E. Zaccarelli, *Phys. Rev. Lett.* **95**, 157802 (2005).

30. A. J. Moreno, I. Saika-Voivod, E. Zaccarelli, E. La Nave, S. V. Buldyrev, P. Tartaglia, and F. Sciortino, *J. Chem. Phys.* **124**, 204509 (2006).

31. M. S. Shell, P. G. Debenedetti, and A. Z. Panagiotopoulos, *Phys. Rev. E* **66**, 011202 (2002).

32. I. Saika-Voivod, F. Sciortino, T. Grande, and P. H. Poole, *Phys. Rev. E* **70**, 061507 (2001).

33. C. A. Angell, *Annu. Rev. Phys. Chem.* **55**, 559 (2004).

34. P. H. Poole, I. Saika-Voivod, and F. Sciortino, *J. Phys. Condens. Matter* **17**, L431 (2005).

35. D. Liu, Y. Zhang, C.-C. Chen, C.-Y. Mou, P. H. Poole, and S.-H. Chen, *Proc. Natl. Acad. Sci. USA* **104**, 9570 (2007).

36. Y. Liu, A. Z. Panagiotopoulos, and P. G. Debenedetti, *J. Chem. Phys.* **131**, 104508 (2009).

37. D. T. Limmer and D. Chandler, *J. Chem. Phys.* **135**, 134503 (2011).

38. I. Saika-Voivod, F. Sciortino, T. Grande, and P. H. Poole, *Phil. Trans. R. Soc. A* **363**, 525 (2005).

39. M. J. Cuthbertson and P. H. Poole, *Phys. Rev. Lett.* **106**, 115706 (2011).

40. M. Hemmati, C. T. Moynihan, and C. A. Angell, *J. Chem. Phys.* **115**, 6663 (2001).

41. M. Agarwal, R. Sharma, and C. Chakravarty, *J. Chem. Phys.* **127**, 164502 (2007).

42. S. Sastry, P. G. Debenedetti, F. Sciortino, and H. E. Stanley, *Phys. Rev. E* **53**, 6144 (1996).